

Journal of Materials Chemistry B

Accepted Manuscript



This is an *Accepted Manuscript*, which has been through the Royal Society of Chemistry peer review process and has been accepted for publication.

Accepted Manuscripts are published online shortly after acceptance, before technical editing, formatting and proof reading. Using this free service, authors can make their results available to the community, in citable form, before we publish the edited article. We will replace this *Accepted Manuscript* with the edited and formatted *Advance Article* as soon as it is available.

You can find more information about *Accepted Manuscripts* in the [Information for Authors](#).

Please note that technical editing may introduce minor changes to the text and/or graphics, which may alter content. The journal's standard [Terms & Conditions](#) and the [Ethical guidelines](#) still apply. In no event shall the Royal Society of Chemistry be held responsible for any errors or omissions in this *Accepted Manuscript* or any consequences arising from the use of any information it contains.

ARTICLE

Biocompatible and antifouling coating of cell membrane phosphorylcholine and mussel catechol modified multi-arm PEGs

Cite this: DOI: 10.1039/x0xx00000x

Yuan Dang, Miao Quan, Cheng-Mei Xing, Yan-Bing Wang and Yong-Kuan Gong*

Received 00th January 2012,
Accepted 00th January 2012

DOI: 10.1039/x0xx00000x

www.rsc.org/

The design and easy fabrication of biocompatible and antifouling coating on different materials are extremely important for biotechnological and biomedical devices. Here we report a substrate-independent biomimetic modification strategy for fabricating biocompatible and antifouling ultra-thin coating. Cell membrane antifouling phosphorylcholine (PC) and/or mussel adhesive catechol (c) groups are grafted at the amino-ends of an 8-armed poly(ethylene glycol). The PC groups are introduced by grafting a random copolymer bearing both PC and active ester groups. The modified 8-arm PEGs (PEG-2c-23PC, PEG-6c-23PC and PEG-8c) anchor themselves onto various substrates from aqueous solution and form cell outer membrane mimetic surfaces. Static contact angle, atomic force microscope (AFM) and X-ray photoelectron spectra (XPS) measurements confirm the successful fabrication of coatings on polydopamine (PDA) precoated surfaces. Real-time interaction results between proteins/bacteria and the coatings measured by surface plasmon resonance (SPR) technique suggest excellent anti-protein adsorption and short-term anti-bacteria adhesion performance. The long-term bacteria adhesion, platelet and L929 cell attachment results strongly support the SPR conclusions. Furthermore, the cell membrane mimetic and mussel adhesive protein mimetic PEG-2c-23PC shows hardly any toxicity to L929 fibroblasts, and the coating surface demonstrates the best anti-biofouling performance. This PDA-assisted immobilization of PC and/or catechol modified multi-arm PEGs provides a convenient and universal way to produce a biocompatible and fouling-resistant surface with tailor-made functions, which hopefully can be expanded to a wider range of applications based on both the structure and surface superiorities.

1. Introduction

Surface modification with hydrophilic polymers such as poly(ethylene glycol) (PEG)^{1,2} and zwitterionic polymers such as poly(carboxybetaine)³⁻⁵, poly(sulfobetaine)⁶⁻⁸ and poly(2-methacryloyloxyethyl phosphorylcholine)^{9,10} is an effective method to improve the biocompatibility and prevent biofouling of a material. Surface immobilization of PEG onto biomedical materials is most widely used to minimize the adhesion of unwanted biomolecules and microorganisms. It is known that PEGylated surface exhibit a stealth effect by repelling protein adsorption and cell adhesion due to the large hydrodynamic volume caused by bound water molecules.¹¹ Jeon *et al.* reported that the anti-biofouling performance of the PEGylated surface greatly depended on the surface density of the grafted PEG.¹² In order to construct high-density PEG surfaces, multi-arm PEGs drew more and more concerns.^{13,14} Once an arm of the branched PEG is adhered to the substrate, the entire polymer is fixed in the meanwhile, providing a facile method to increase

the PEG density covered on the surface. Moreover, the multi-arm PEG provides more modifiable sites to make the PEG coatings multifunctional.

Phosphorylcholine (PC) is the hydrophilic head group of cell outer membrane phosphatidylcholine and endows the cell membrane ideal biocompatibility, especially in resistance to protein adsorption and cell adhesion.^{15,16} The migration and reorientation of the PC groups in aqueous circumstances helps the PC-based zwitterionic surfaces to form a cell outer membrane mimicking structure and effectively suppress the attachment of biofoulers.^{17,18} The protein resistance property of PEG and zwitterionic PC groups could be synergistic. PEG and PC hybrid alkanethiol had a greater suppressive effect on protein adsorption than the corresponding ethylene glycol-alkanethiol.¹⁹ Ishihara *et al.* reported that a PC polymer having an oxyethylene chain as a bridging unit was much more effective in reducing platelet adhesion than a pure phospholipid polymer.²⁰ A hybrid of PEG and PC polymers might be

promising to construct a dual and synergistic fouling-resistant coating.

However, PEG and PC polymers are extremely hydrophilic and hence have high solubility in water, making them difficult to be attached onto a surface. Therefore, specific interaction between the interfacial modifier and the surface is required to immobilize such hydrophilic polymers. Possible interactions include thiolate on noble metals,²¹ phosphonic acid on titanium oxides,²² and organosilane and polyamines on various oxides.²³ These surface-specific interactions restrict the application of PEGylated surfaces to a few given materials. Therefore, the development of simple and versatile methods for surface modification is crucially important for the construction of functional interfaces of advanced materials.²⁴

In recent years, catechol, the essential adhesive group of 3,4-dihydroxy-L-phenylalanine (DOPA) and dopamine (DA) found extensively in mussel-adhesive proteins,²⁵ emerged as a surface-independent anchor molecule and provided a versatile method to bind coatings to material surfaces including hydrophilic, hydrophobic, even fluorine-containing materials.^{26,27} Although this biomimetic strategy can immobilize catechol-containing PEG and PC polymers onto various substrates by increasing the catechol content,^{27,28} the adhesive groups remain on the surface may also bind proteins and cells. Therefore, it is still challenging to fabricate a super-low fouling coating either on a strongly hydrophobic substrate or with a hydrophilic polymer containing low content of catechols. To overcome this dilemma, polydopamine (PDA) mediated surface grafting method²⁶ is worth to be explored further.

In this study, doubly modified 8-arm PEGs were synthesized by grafting different number of cell membrane anti-fouling PC and mussel-inspired catechol anchoring groups to the arm-ends. The doubly functionalized 8-arm PEGs were immobilized from aqueous solution onto various substrates through PDA-mediated chemistry. The coated surfaces showed excellent resistance to the adsorption/adhesion of protein, platelets, fibroblast cells and bacteria.

2. Experimental Section

2.1 Chemicals.

2-Methacryloxyethyl phosphorylcholine (MPC) and p-nitrophenoxycarbonyloxyethyl methacrylate (NPCEMA) were synthesized according to the methods reported by Ishihara²⁹ and Konno³⁰. The initiator 2,2'-Azobis-(2,4-dimethylvalero-nitrile) (AVBN, from J&K Co.) was used as received. 8-arm PEG amine ($M_w \sim 10,000$ g/mol) was purchased from Nanotech. 3-(3,4-dihydroxyphenyl)propionic acid (DHPA, 98%) was obtained from Alfa Aesar and used as received. N-hydroxybenzotriazole (HOBt) and O-benzotriazole-N,N,N',N'-tetramethyl-uronium-hexafluoro-phosphate (HBTU) from J&K Co. were used without further purification. Bovine serum albumin (BSA) and bovine plasma fibrinogen (Fg) were purchased from Sigma-Aldrich. Water used was purified using a Millipore water purification system with a minimum

resistivity of 18.2 M Ω .cm. All other chemicals were analytical reagents grade and were used without further purification unless otherwise indicated.

2.2 Synthesis of PC and/or catechol end-capped 8-arm PEG.

Random copolymer bearing both PC and active ester side chains (PMEN) was synthesized by conventional free-radical copolymerization of MPC and NPCEMA with a molar ratio of 80:20. The MPC and NPCEMA unit mole fractions of the PMEN were estimated to be 0.75 and 0.25 respectively by ¹H NMR measurement with an Inova 400 NMR spectrometer (Varian, USA), shown in Fig. S1. The molecular weight of PMEN was characterized to be $M_w \sim 6000$ g/mol by an aqueous gel permeation chromatograph (GPC) (Dionex Ultimate 3000) with a Sheodex RI-101 refractive index detector and a Sheodex OHPak SB-803 column (8 \times 300 mm²). Aqueous solution of sodium azide (0.02%) was used as the eluent with a flow rate of 1.0 ml/min at 40°C. The system was calibrated with narrow-molecular-weight poly(ethylene oxide) standards.

Then, 0.3 mmol PMEN dissolved in ethanol was dropped into 0.2 mmol 8-arm PEG amine solution in ethanol:water = 9:1 (v/v) mixed solvent. The pH of the reaction solution was adjusted around 7 by triethylamine to provide an easier atmosphere for the amidation coupling between the end-capped amine groups in the 8-arm PEG and active ester groups in PMEN. The reaction was kept at 60°C for 24 hours. After the amidation was finished, the pH of the reaction solution was adjusted to 9 and stirred for another 2 hours at room temperature to hydrolyze the unreacted p-nitrophenyl ester groups in the grafted PMEN. Then, the resulting PEG-g-(PMEN)_m-(NH₂)_{8-m} was dialyzed against water using an MWCO 12000 g/mol dialysis tube and lyophilized. The grafted amount of PMEN was determined by ¹H NMR and GPC.

The grafting of catechol groups onto the PEG-g-(PMEN)_m-(NH₂)_{8-m} was carried out as the following procedures. Under the protection of nitrogen atmosphere, DHPA, HBTU, HOBt and triethylamine in a molar ratio of 1:1:1.65:1.65 were added to dichloromethane/N,N-dimethylformamide mixed solvent (1/1, v/v) containing PEG-g-(PMEN)_m-(NH₂)_{8-m}. After 12 hours of reaction, the solution was filtered and precipitated in cold diethyl ether. The product was dried under vacuum and resuspended in aqueous solution at pH 4.0, followed by dialysis against acidic water for 72 hours. After freeze drying, the number of the grafted catechols in the PC and catechol end-capped 8-arm PEG (doubly biomimetic 8-arm PEGs) was determined by UV-Vis spectrometry. Gradient concentrations of DHPA (0.025~5 \times 10⁻⁴ mol/l) were prepared in pH 4.0 buffer to establish the standard curve of catechol concentration versus the UV absorbance at 280 nm with a Lambda 40P UV-Vis Spectrometer. The catechol content of the modified 8-arm PEG polymers was calculated from the DHPA standard curve.

2.3 Surface modification.

Gold, glass, polycarbonate, steel and polytetrafluoroethylene (PTFE) substrates were selected for surface modification. The detergent-washed substrates were rinsed with ethanol and pure water, and then dried in a stream of dry nitrogen prior to use. The surface modification consisted of the following steps:

Firstly, clean substrates were immersed in a dopamine solution (0.5 mg/ml in 10 mM Tris-HCl, pH 8.5) for 6 hours at room temperature. The PDA precoated substrates were washed with ultrapure water and dried with nitrogen gas. Then, the modified 8-arm PEGs were coated onto the PDA precoated substrates by immersing, drop or spin coating with 0.5 mg/ml solution in ethanol:water=50:50 (v/v) mixed solvent. After heated at 110°C for 10 hours, the samples were immersed in stirred water for 4 hours to wash away the loosely adsorbed polymers. The coated substrates were further immersed in 80°C water for 30 min to reconstruct the biomimetic PEG coating to more hydrophilic state. Finally, the prepared surfaces were dried with nitrogen gas before use.

Moreover, the biomimetic 8-arm PEG polymer solution (in Tris-HCl, pH 8.5) was also injected over a surface plasmon resonance (SPR) sensor chip to monitor the automatic immobilization process in real time.

2.4 Static contact angle measurement.

The static contact angles of water on the uncoated or polymer-coated substrates were measured with a video-based OCA 20 contact angle goniometer (Dataphysics, Germany). Ultrapure water (5 μ l) was used for the measurements. All samples were analyzed in triplicate.

2.5 Surface elemental analysis.

The elemental composition of the uncoated and coated surfaces was determined by X-ray photoelectron spectroscopy (XPS) (K-Alpha, Thermo Electron Corporation, USA) using monochromatic Al K radiation (200 W, 12 KV, 1486.68 eV). The vacuum in the spectrometer was kept at 10^{-7} Pa. All spectra were collected at an electron take-off angle of 90° from the surface. Binding energies were calibrated relative to the C1s peak (284.8 eV) from hydrocarbons adsorbed on the surface of the samples. The high-resolution N1s and P2p spectra were fitted using a Shirley background subtraction and a series of Gaussian peaks using the XPSPEAK software.

2.6 Morphology.

The morphological analysis of the studied surfaces in air and liquid (ultrapure water) environments was performed using a Multi Mode 8 atomic force microscope (Bruker, USA). Silicon tips on nitride cantilever from Bruker were utilized with SCANASYST Mode in air or fluid. The spring constant (k) was 0.4 N/m in air or 0.7 N/m in fluid. The sample was attached to the magnetic stainless steel disc which was immobilized on the AFM machine without movement. $1 \times 1 \mu\text{m}^2$ randomly chosen areas were scanned at a scan frequency of 0.996 Hz using a $125 \times 125 \mu\text{m}^2$ type piezo scanner to obtain the topography of the surfaces.

2.7 Thickness measurement.

The coating thickness was measured on a quartz substrate for its prominent hardness. The deposited polymer coating on the quartz substrates was partially shaved by knife-scratching the surface under a suitable force to create a piece of bare quartz surface in order to establish a zero point (0 nm) for thickness measurements. Subsequently, at least three adjacent areas of $40 \times 40 \mu\text{m}^2$ were scanned using a Multi Mode 8 AFM with SCANASYST Mode. The coating thickness was calculated

from the average height obtained in the shaved area and an adjacent unshaved area via the Bruker NanoScope Analysis software.

2.8 Protein adsorption.

Nonspecific protein adsorption on the modified 8-arm PEG coatings was evaluated with a Reichert SR7500DC Dual Channel surface plasmon resonance (SPR) System (Reichert, USA). The modified SPR sensor chip was attached to the base of the prism. The adsorption of biomolecules to the sensor surface resulted in a shift in the refractive index that was reported in μ RIU units. The change in μ RIU units as a function of time was monitored in real time using the Integrated SPRAutolink software program. The data were plotted using Origin 8.0 software program to give a sensorgram profile.

The nonspecific protein adsorption was operated in a flow-through mode with a flow rate of 50 μ l/min at 25°C. Briefly, the operation protocol is as follows: (a) passing the degassed PBS buffer over the chip for at least 10 min to obtain a stable baseline; (b) delivering 1 mg/ml bovine serum albumin (BSA) or fibrinogen (Fg) in PBS over sensor chip surface for 10 min; (c) then rinsing the surface with PBS buffer for about 30 min to wash off the loosely adsorbed protein and reach a steady-state value. The adsorbed amount of protein was evaluated by the baseline difference given in response units before and after exposure of the chip surface to the protein solution.

2.9 Platelet attachment.

The platelet attachment test of the modified surfaces was performed under static conditions according to a previously reported method.³¹ Blood collection and platelet experiments were approved by the Institutional Review Board of Northwest University, and all the experiments were performed in compliance with the relevant laws and institutional guidelines. Fresh whole blood was donated by a 25-year-old healthy male and collected in a polyethylene disposable syringe containing 3.8 wt % aqueous sodium citrate solution. The citrated whole blood was immediately centrifuged for 10 min at 1000 rpm to obtain platelet-rich plasma (PRP). The sample surfaces were placed in petri dishes and equilibrated by immersion in PBS for 2 hours. Subsequently, 20 μ l fresh PRP was dropped on the center of each sample surface and incubated at 37°C for 2 hours in a humidified water jacketed incubator equilibrated with 5% CO₂ in air. Afterwards, the samples were rinsed with PBS to remove the weakly adhered platelets and the remaining adherent platelets are fixed in 2.5 wt% glutaraldehyde solution for 1 hour. After rinsing several times with PBS solution and ultrapure water, the fixed samples were lyophilized overnight and observed with an FEI QUANTA 600 FEG SEM.

2.10 L929 cell viability.

A tetrazolium-based assay was used to quantify the cytotoxicity of the modified 8-arm PEGs according to the method of Mosmann *et al.*³² L929 mammalian fibroblast cells used in this study were first cultured at 37°C with 5% CO₂ in Dulbecco's Modified Eagle Media (DMEM) supplemented with 10% Fetal Bovine Serum (FBS) and 100 U/ml of penicillin/streptomycin. They were harvested using 0.25% trypsin-EDTA, counted using a hemacytometer immediately before use, and

resuspended in the cell culture media at a concentration of 5×10^4 cells/ml. The cell suspension was plated into 96-well microtiter plates (Nunc). After 24 hours, culture medium was replaced by 100 μ l serial dilutions of the polymers (0.05 to 1.00 mg/ml) dissolved in 10% FBS supplemented DMEM and sterilized by filtration (0.2 μ m). The cells were incubated for 24 and 48 hours. Polymer solutions were aspirated and PBS was added to wash off the dead cells. Then 20 μ l sterile filtered (3-(4,5-dimethylthiazol-2-yl)-2,5-diphenyl tetrazolium bromide) (MTT, sigma) stock solution in PBS (5 mg/ml) were added to each well. After incubation at 37°C for 4 hours, MTT was removed and 200 μ l/well DMSO was added for 10 min to dissolve reduced formazan crystals. The optical density of the formazan solution was then measured spectrophotometrically at a wavelength of 490 nm (test) and 630 nm (reference) using an ELISA plate reader. Control experiments were carried out under the same condition except that no polymers were added during cell culture processes. Each treatment condition with the modified PEGs or control agents was assessed in six copies. The relative cell viability (%) related to control wells was calculated by $[\text{OD}]_{\text{test}}/[\text{OD}]_{\text{control}} \times 100$.

2.11 L929 cell adhesion.

The cell adhesion test was performed using L929 cells on the PEGs-modified glass substrate. L929 mammalian fibroblast cells were freshly harvested and resuspended in the cell culture media at a concentration of 5×10^4 cells/ml. The modified and virgin glass substrates (10 \times 10 mm²) were placed in 24-well culture plates and sterilized by UV irradiation for 30 min. After equilibrated in PBS for 2 hours, 2 ml/well L929 fibroblast cells suspension in 10% FBS supplemented DMEM was added to replace PBS. The surfaces were then incubated at 37°C and 5% CO₂ for 1, 3 and 7 days. Subsequently, the medium was aspirated from each well and PBS was used to rinse the substrates and wells to remove any non-adherent cells. The adhered fibroblasts were stained with 20 μ l/well Syto9 in PBS (2 μ l/ml) for 20 min and the substrates were transferred to new culture plates with PBS buffer. For the 7 days' adhesion experiments, the surfaces were reseeded with L929 on the third day after changing the media. Three random locations on each surface were observed using inverted fluorescence microscope (Ti-U, Nikon) and quantified using threshold analysis in ImageJ software.

2.12 Bacteria adhesion.

Bacteria adhesion on the virgin and modified substrates was assessed by *Escherichia coli* (*E. coli*), *Staphylococcus aureus* (*S. aureus*) and *Pseudomonas aeruginosa* (*P. aeruginosa*) attachments from a suspension of 5×10^7 cells/ml in PBS. The short-term (2 hours) attachment was monitored in real time with a SR7500DC SPR system. The operation process of SPR method was similar to that of the protein adsorption. Firstly, flushing the SPR sensor chip surface with PBS to get a stable baseline with a flow rate of 10 μ l/min at 37°C. Subsequently, the freshly suspended bacteria solution was pumped into the channels for 2 hours to give SPR profile of the bacteria attachment. Finally, replacing the bacteria solution with PBS and reaching a steady-state value. The amount of adhered

bacteria was expressed as the baseline difference measured in PBS before and after contact with the bacteria solution.

The long-term (7 days) bacteria adhesion property was evaluated by fluorescent staining method according to the method of Fullenkamp *et al.*³³ For convenience, the long-term bacteria adhesion was evaluated on glass substrates. The modified and virgin glass substrates (10 \times 10 mm²) were placed into 24-well cell culture plates, sterilized by exposure to UV light for 30 min and then equilibrated with sterilized PBS for 2 hours. After replacing the PBS with the freshly prepared bacteria suspension, the samples were incubated at 37°C for 1, 3 and 7 days. Fresh bacteria suspension was seeded into the wells to substitute the old one every day. After finishing the cultivation, the surfaces were rinsed with PBS to remove loosely adhered bacteria. The attached bacteria were then stained with Syto9 (2 μ l/ml) in PBS and visualized using an Olympus FV1000 confocal microscope (with a 20 \times objective lens). Three identical surfaces for each experiment were analyzed for statistical purpose. The microscopy images were quantified using threshold analysis in ImageJ software.

2.13 Statistical analysis.

All results were expressed as mean values \pm standard deviation (SD). The statistical significance of differences between mean values was determined by using a t-test and ANOVA for analysis of variance. Values of $p < 0.05$ were considered statistically significant.

3. Results and Discussion

3.1 Synthesis and characterization of PC and/or catechol end-capped 8-arm PEG.

The amidation coupling reaction between p-nitrophenyl-oxy carbonyl groups in PMEN and primary amine groups in the 8-arm PEG amine facilitated the grafting of PC-containing random copolymer PMEN to the branched PEG. The appearance of the typical PC signal at $\delta = 3.28$ in the ¹H NMR spectrum of the purified product affirmed the successful coupling of PMEN with the 8-arm PEG amine. The PMEN content in the grafted 8-arm PEG (PEG-g-PMEN) was calculated by the molecular weight change based on the GPC results. The molecular weight (M_w) shifted from $\sim 10,000$ g/mol of the 8-arm PEG amine to $\sim 19,500$ g/mol after grafting PMEN ($\sim 6,000$ g/mol), indicated that about 1.5 mol PMEN (23 mol PC groups) was grafted to 1 mol of the 8-arm PEG amine (PEG-g-(PMEN)_{1.5}). Although any of the active ester groups at the PMEN oligomer could be involved in the coupling, usually only one of them was coupled since the remaining active ester groups were far away from the other amine groups. This analysis was supported by coupling almost all the remaining amine groups of PEG-g-(PMEN)_{1.5} with the adhesive catechol molecules. As shown in Fig. 1, the multiple peak at $\delta = 6.40$ -7.30 was attributed to the protons on benzene skeleton of catechol groups, implying that DHPA was successfully tethered onto the 8-arm PEG. Based on the GPC results, the grafting degree of catechol groups onto the 8-arm PEG amine was determined via interpolation of the absorption of the catechol polymer

solutions against the DHPA standard curve at 280 nm. By changing the feeding molar ratio of DHPA and 8-arm PEG amine, we obtained three kinds of doubly biomimetic 8-arm PEGs, (catechol)_{2.5}-g-PEG-g-(PMEN)_{1.5}-(NH₂)₄, (catechol)_{6.0}-g-PEG-g-(PMEN)_{1.5}-(NH₂)_{0.5} and PEG-g-(catechol)₈, simplified as PEG-2c-23PC, PEG-6c-23PC and PEG-8c respectively. The characterization results of the biomimetic 8-arm PEGs were shown in Table 1.

3.2 Coating formation and characterization.

The PC and/or catechol modified 8-arm PEG polymers were highly water-soluble. It was challenging to immobilize them onto various substrates from aqueous solution. As shown in Fig. 2, although the self-adhesive PEG-2c-23PC, PEG-6c-23PC and PEG-8c polymers could adhere themselves on the gold chip surface, the coating formation was slow and the adhered amount of the polymers was limited, especially for PEG-2c-23PC with the minimal catechol groups. On the surface of PDA pre-coated chips, the rate of coating thickness growth was significantly improved and the amount of adhered polymers increased by 214%, 97% and 79% for PEG-2c-23PC, PEG-6c-23PC and PEG-8c respectively. Obviously, the introduction of PDA composite layer facilitated the anchoring of the highly hydrophilic modified PEGs, particularly for catechol-limited PEG-2c-23PC. This phenomenon was consistent with previous reports by Sundaram *et al.*³⁴, possibly resulted from the further oxidation and cross-linking between PDA coating and the end-capped catechol groups of the modified multi-arm PEGs.

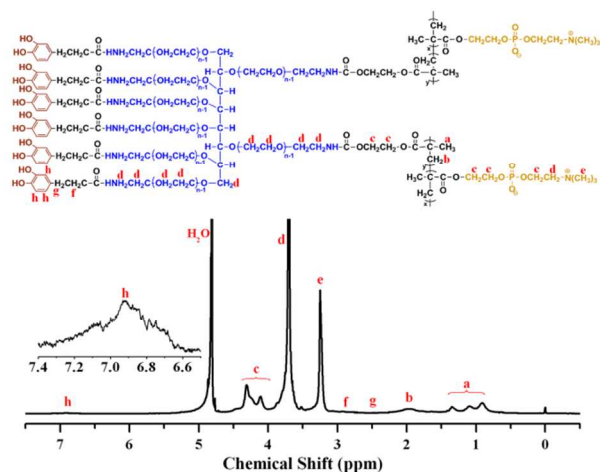


Fig. 1 The ¹H NMR spectra of PC and catechol end-capped 8-arm PEG (PEG-6c-23PC, s: D₂O)

Table 1 Characterization results of PC and/or catechol end-capped 8-arm PEG

Sample	Molecular weight [M _w , g/mol] ^(a)	PDI	PMEN content [mol%] ^(b)	Catechol content [mol%] ^(c)
PEG-2c-23PC	20050	1.31	1.58	2.48
PEG-6c-23PC	21980	1.43	1.58	5.92
PEG-8c	11370	1.11	0	7.82

^(a) Determined by means of GPC. ^(b) The PMEN and catechol contents were molar ratios to PEG and calculated from the molecular weight change before and after grafting PMEN. ^(c) Obtained by UV-Vis characterization at 280 nm.

On the basis of the above results and previous findings, we turned to fabricate the PC and/or catechol modified 8-arm PEG coatings on various substrates assisted by PDA sublayer, which could be formed automatically from aqueous solution of dopamine onto material independent substrates.²⁶ The modified 8-arm PEG dissolved in mixed water/ethanol (1/1, v/v) solution was spin-coated on the PDA pre-coated substrates. To accelerate the oxidation and crosslinking reactions of the catechol groups and stabilize the coatings, the coated substrates were heated in air at 110°C for 10 hours. Immersion in 80°C water for 30 min allowed for the surface reconstruction and formation of cell outer membrane mimetic structure,^{17,18} constituting the second resistant screen for biofouling on the main antifouling layer of the 8-arm PEG. Static water contact angle, X-ray photoelectron spectroscopy (XPS) and atomic force microscope (AFM) results on gold, glass, polycarbonate, steel and polytetrafluoroethylene were collected to assess the general applicability

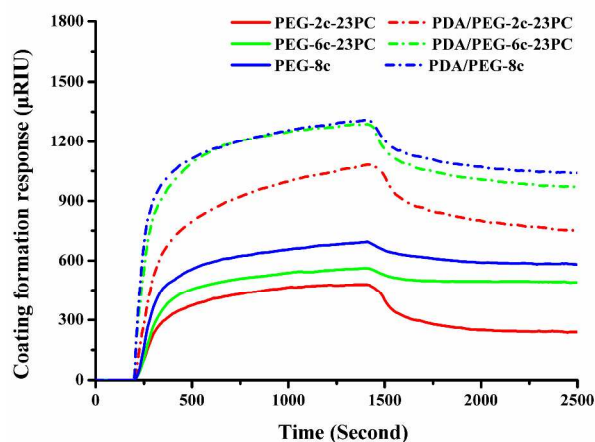


Fig. 2 The typical SPR sensorgrams of the modified 8-arm PEG coating formation with/without PDA-mediated layer on the sensor chip surface. The doubly biomimetic 8-arm PEGs, dissolved in tris(hydroxymethyl)amino-methane (Tris) buffer (pH 8.5), was passed through the SPR sensor chips at a rate of 10 µl/min for 20 min to get the real-time deposition curves.

Table 2 Static contact angle and XPS N1s and P2p spectra of the virgin and spin-coated films on gold substrate

Sample	Static contact angle (°)	XPS spectra in N1s and P2p regions	
		N1s	P2p
Virgin gold	101.1±0.5		
PDA	67.3±1.4		
PDA/PEG-2c-23PC	43.2±0.8		
PDA/PEG-6c-23PC	46.7±0.8		
PDA/PEG-8c	48.4±0.7		

of the strategy. Represented by gold substrate, the characterization results of the coatings were listed in Table 2 and Fig. 3. The coating information on other substrates could be found in Fig. S2, which confirms the versatility of the PDA-assisted immobilization for the modified 8-arm PEGs.

Static water contact angle was measured to examine the surface hydrophilicity. As listed in Table 2, the uncoated gold surface was $101.1 \pm 0.5^\circ$, indicating a hydrophobic surface. After coated with polydopamine (PDA), the contact angle was reduced to $67.3 \pm 1.4^\circ$. When PEG-2c-23PC, PEG-6c-23PC and PEG-8c coatings were immobilized onto the PDA surface, the static contact angles were further decreased to $43.2 \pm 0.8^\circ$, $46.7 \pm 0.8^\circ$ and $48.4 \pm 0.7^\circ$ respectively. The obvious decrease in the contact angles indicated that the surface hydrophilicity was improved and the coating construction was successful. Moreover, the small difference in contact angles of the modified PEG surfaces could be ascribed to the composition difference of polymers after completely covered the substrate.

Furthermore, elemental composition analysis on the modified surfaces provided more direct evidence for the successful coating formation. Table 2 showed the typical XPS high resolution spectra of N1s and P2p at different steps of coating-fabrication. The peaks of secondary amine groups at 399.8 eV confirmed the PDA film deposition on the substrate surfaces. The appearance of new N1s peak at 402.6 eV and P2p peak at

133.3 eV indicated the existence of PC groups, which strongly supported the successful immobilization of the doubly biomimetic 8-arm PEGs (PEG-2c-23PC and PEG-6c-23PC) on the PDA coated gold chips.

AFM 2D and 3D images were collected to study the morphology and nanostructure of the coating surfaces in air, as shown in Fig. 3. While the virgin and PDA coated gold surface appeared fairly smooth with small and equally distributed features, the biomimetic 8-arm PEG coatings showed unevenly distributed broader features. The roughness of the surfaces was assessed by measuring roughness parameter, R_q (root mean square roughness). The slightly higher R_q roughness of PDA surface (0.782 nm) and bigger topographic features than the virgin gold (R_q roughness = 0.626 nm) suggested the PDA film formation. After coupling of the biomimetic 8-arm PEGs on PDA coating, the surface R_q in air increased significantly to 2.44 nm, 2.19 nm and 2.27 nm for PEG-2c-23PC, PEG-6c-23PC and PEG-8c surfaces, respectively. These results further supported the successful fabrication of PEG-2c-23PC, PEG-6c-23PC and PEG-8c coatings on the basis of PDA composite interfaces. The microstructures of the biomimetic 8-arm PEG coatings might be affected by the competition between the self-crosslinking of catechol groups tethered on the modified PEGs and their anchoring reaction with surface catechols of the PDA sublayer. The big aggregates on the PDA/PEG-2c-23PC surface were possibly due to fewer crosslinking among the polymers. Dynamic light scattering result suggested that the PEG-8c aggregates formed in solution might be responsible for the morphology of PDA/PEG-8c surface. As for PDA/PEG-6c-23PC, the adequate catechol groups and strong hydration capacity promoted the self-crosslinking of the polymers, resulting in slightly smaller clusters.

The thickness of the dry and hydrated coatings measured by AFM images was listed in Table 3. The increased thickness in dry state further confirmed the formation of PDA and biomimetic 8-arm PEG coatings. The thickness of the biomimetic PEG coatings was correlated to the amount of their end-capped catechol groups. The more content of catechol

Table 3 Coating thickness and R_q roughness of spin-coated films measured by AFM

Sample	Thickness in air (nm) ^(a)	Thickness in fluid (nm) ^(a)	Swelling ratio ^(b)	R_q roughness (nm) ^(c)
Virgin gold	–	–	–	0.626
PDA	6.9 ± 0.8	15.4 ± 0.9	123%	0.782
PDA/PEG-2c-23PC	10.8 ± 0.5	22.7 ± 0.6	87%	2.44
PDA/PEG-6c-23PC	15.4 ± 0.5	28.7 ± 0.9	56%	2.19
PDA/PEG-8c	15.8 ± 0.5	27.3 ± 0.5	34%	2.27

^(a) By measuring the height difference between the shaven and unshaven portions of the surfaces. ^(b) Calculated from the swelled thickness increment of the individual layer PDA or biomimetic 8-arm PEGs by subtracting the sublayer effect. ^(c) R_q roughness, expressed as

$R_q = \sqrt{\frac{1}{N} \sum_{i=1}^N (h_i - \bar{h})^2}$. Here, h_i is the current height value, \bar{h} the height of the mean data plane, and N the number of points within the box cursor.

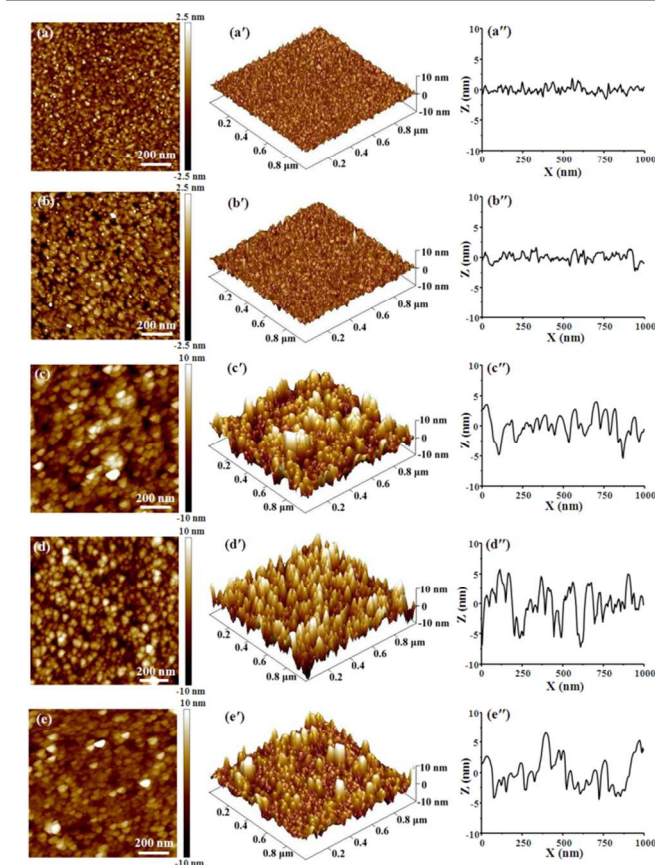


Fig. 3 AFM 2D, 3D images and section plots of $1 \mu\text{m}^2$ scans for polymer spin-coated surfaces in air. (a) Virgin gold; (b) PDA coated gold; (c) PDA/PEG-2c-23PC coated gold; (d) PDA/PEG-6c-23PC coated gold; (e) PDA/PEG-8c coated gold.

groups within the PEGs, the thicker coating formation. This phenomenon was mainly attributed to the adhesive function of catechol. The small thickness of the individual multi-arm PEG coatings (3.9~8.9 nm) was probably limited to monolayer formation of the modified PEGs. The strong hydrophilicity, surface anchoring and possible crosslinking of the modified PEGs restricted the further growing of the coatings. The highest swelling ratio of PEG-2c-23PC coating (87%) among the PEG films shown in Table 3 can be ascribed to the lowest crosslink degree and the most freedom of water adsorbing PEG-2c-23PC structure.

3.3 Biocompatibility and anti-biofouling evaluation.

The simply formed PC and/or catechol grafted 8-arm PEG coatings were expected to be biocompatible and biofouling resistance. Their biocompatibility and anti-biofouling properties were evaluated by protein adsorption, platelet, bacteria and fibroblast cell adhesions, and cell viability measurements.

3.3.1 Protein adsorption.

Protein resistance property of the spin-coated 8-arm PEG surfaces was monitored by SPR method using BSA and Fg as model proteins. Fig. 4 showed typical SPR sensorgrams of protein adsorption from 1 mg/ml BSA and Fg solutions onto the different surfaces. As expected, the amount of adsorbed protein on the pristine gold surface was as high as 96.9 ng/cm² for BSA and 300 ng/cm² for Fg due to the hydrophobic-hydrophobic interaction between the gold and protein molecules (1 μ RIU = 0.1 ng/cm²).³⁵ The adsorbed BSA and Fg was reduced in some extent on the PDA coated surface because of the repulsive forces of the hydrophilic PDA surface. However, the benzene

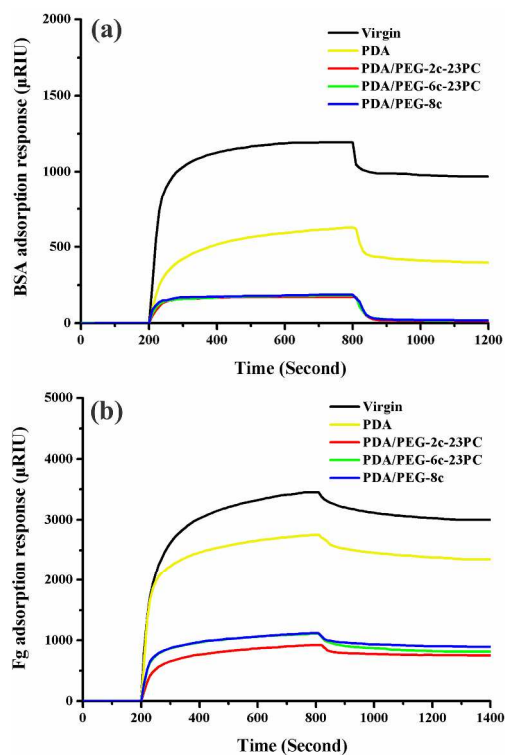


Fig. 4 SPR sensorgrams of protein adsorption from 1 mg/ml BSA and Fg solutions onto unmodified and modified gold chips. (a) BSA adsorption; (b) Fg adsorption.

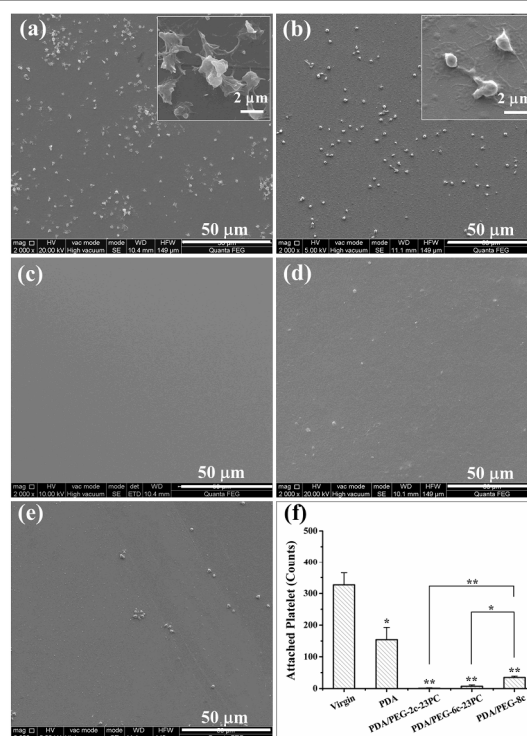


Fig. 5 SEM images of platelet adhesion from platelet-rich plasma (PRP) on the virgin (a), PDA coated (b), PDA/PEG-2c-23PC coated (c), PDA/PEG-6c-23PC coated (d), and PDA/PEG-8c coated (e) gold surfaces, (f) Amount of adhered platelets on different surfaces counted on 0.3×0.3 mm² scales. **p*≤0.05 and ***p*≤0.01 versus the adhered platelets on the virgin chip or the corresponding reference surface, respectively.

rings and possible π - π stacking structure of PDA might attract proteins.^{36,37} Compared to the virgin and PDA coated gold surfaces, PC and/or catechol end-capped 8-arm PEG coatings could significantly suppress BSA and Fg adsorption. PEG-2c-23PC showed the most excellent protein resistance property among the three modified 8-arm PEGs, resisting 98.7% and 75.1% of protein adsorption for BSA and Fg respectively compared to the virgin gold surface. The doubly biomimetic 8-arm PEGs (PEG-2c-23PC and PEG-6c-23PC) showed stronger suppression to protein adsorption probably due to their cell membrane mimetic structure of the zwitterionic PC groups.^{19,20}

3.3.2 Platelet attachment.

Anti-platelet adhesion capacity is one of the main research targets to biomedical materials for its close relationship to thrombotic events.³⁸ Fig. 5 showed the respective SEM images and quantitative analysis of platelets attached on the differently modified gold surfaces. SEM images of 2000× magnification clearly showed that a significant amount of platelets adhered and spread on the virgin gold surface (Fig. 5a). Whereas, platelets incubated on the modified PEG coatings displayed only a few attachments, suppressing more than 90% of platelet adhesion compared to the virgin gold surface. More excitingly, platelet adhesion was completely prevented on the surface of PDA/PEG-2c-23PC coating.

It was reported that platelet adhesion and activation were closely related to adsorbed fibrinogen and the threshold value

was 20 ng/cm².³⁹ As shown in Fig. 4b, the amount of adsorbed Fg onto the PDA/PEG-2c-23PC coating was about 74.7 ng/cm², which was much larger than the reported threshold value. The high concentration of the adsorbed Fg on the PDA/PEG-2c-23PC surface did not activate and promote platelet adhesion, suggesting the adsorbed proteins in their native conformation^{40,41} and excellent biocompatibility of the coating.

3.3.3 L929 cell viability and cell attachment.

To further assess the utility of these PC and/or catechol grafted 8-arm PEGs as biomaterials, we studied the cell viability of L929 cultured in different concentrations of polymer solutions for 24 hours and 48 hours by MTT assay. Shown in Fig. 6, an increase in polymer concentrations from 0.05 to 1.00 mg/ml was almost harmless for the cell survival in the cases of PEG-2c-23PC, PEG-6c-23PC and PEG-8c. Above 80% of L929 fibroblasts were alive even in 1 mg/ml polymer solutions cultured for 48 hours (shown in Fig. S3), which was much higher than that of toxic phenol (~30%). As can be seen, the fibroblast viability was not greatly affected by both time points and concentrations of the PEGs solutions. Therefore, the biomimetic PEGs can be used safely as biomedical materials.

Cell attachment response on material surface plays an important role in designing various types of biomedical devices and usually needs to be prevented by proper surface modification. Fig. 7 showed the representative fluorescence images of the virgin and modified glass substrates after the L929 cell adhesion. Contrary to the almost full-scale surface coverage of adhered cells on the bare and PDA coated glass surfaces, less adhered cells were observed on the PC and/or catechol modified PEG coatings at all the time points. The quantitative statistics of the attached L929 fibroblast cells was obtained from ImageJ analysis and shown in Fig. S4. Compared to the virgin glass at each of the time points, the doubly biomimetic PEG coatings suppressed more than 99% L929 attachment. The excellent cell-resistance property of PC grafted PEG-2c-23PC and PEG-6c-23PC surface was significantly superior to that of PEG-8c possibly due to their better hydrophilicity and cell membrane mimetic structure, consistent with the protein- and platelet-resistant results.

3.3.4 Bacteria adhesion.

It is generally accepted that a protein-resistant surface is required to resist subsequent cell and bacteria adhesion, because nonspecific protein adsorption is an instigator for successive foreign body reaction. On the other hand, a surface resisting protein adsorption and cell adhesion does not necessarily imply that this surface can resist bacteria adhesion and biofilm formation.^{42,43} In this work, a Gram positive strain of *S. aureus* and Gram negative strains of *E. coli* and *P. aeruginosa* were used to quantify bacteria adhesion, as they are main pathogen infection in hospitals and major colonizing bacteria on various biomedical implants under a wide range of environmental conditions.

The short-term bacteria adhesion test was conducted on the SPR sensor chips. SPR was used to investigate the dynamic interaction between bacteria and the surfaces in real time under physiological conditions without labeling. The typical SPR sensorgrams of *E. coli*, *P. aeruginosa* and *S. aureus* attachment on the bare and modified gold chips were shown in Fig. 8. It's obvious that the adhered amount of the three most familiar bacteria substantially decreased on the PC and/or catechol end-capped 8-arm PEG coatings compared to the bare gold surface. Although loosely adhered bacteria were difficult to be eluted in

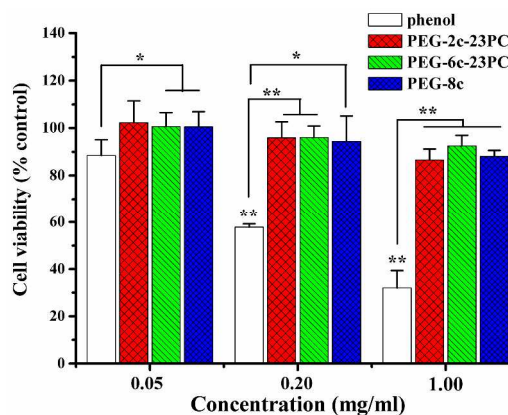


Fig. 6 Relative cell viability of L929 cultured in different concentrations of sample solutions for 24 hours. The cell viability of control group was set as 100%. * $p \leq 0.05$ and ** $p \leq 0.01$ versus that of the control or the phenol group.

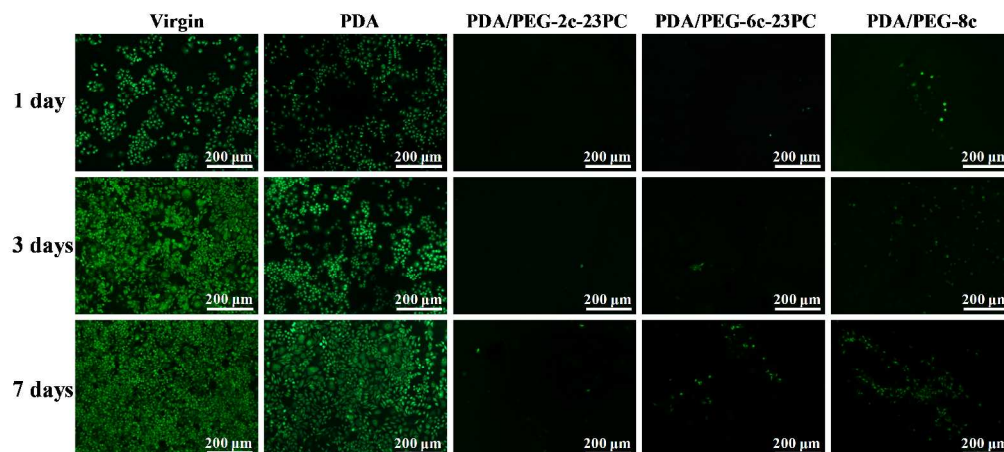


Fig. 7 Fluorescence microscopic images of L929 fibroblast cell adhesion on the modified glass substrates after 1, 3 and 7 days of incubation.

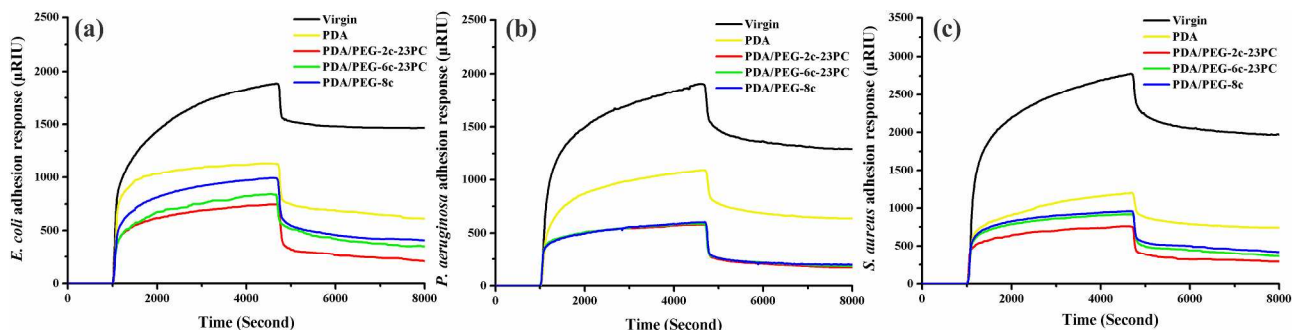


Fig. 8 SPR sensorgrams of short-term bacteria adhesions on the bare and modified gold sensor chips. (a) *E. coli* adhesion; (b) *P. aeruginosa* adhesion; (c) *S. aureus* adhesion.

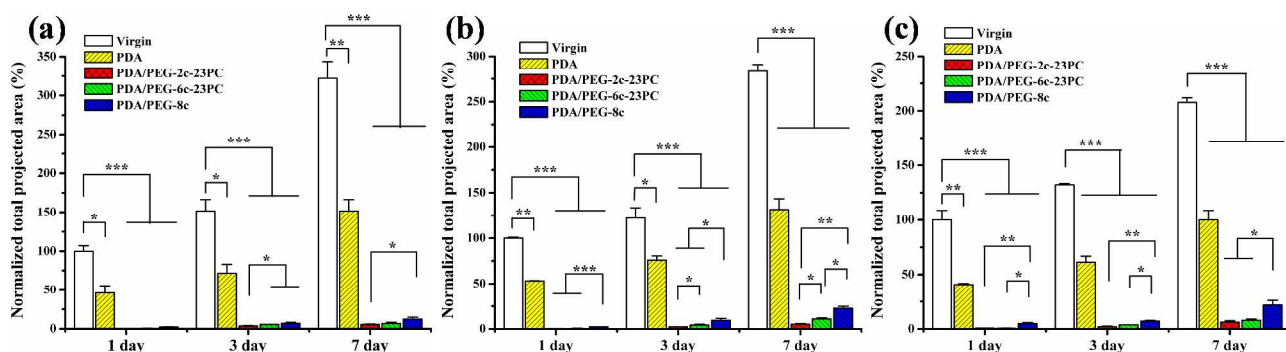
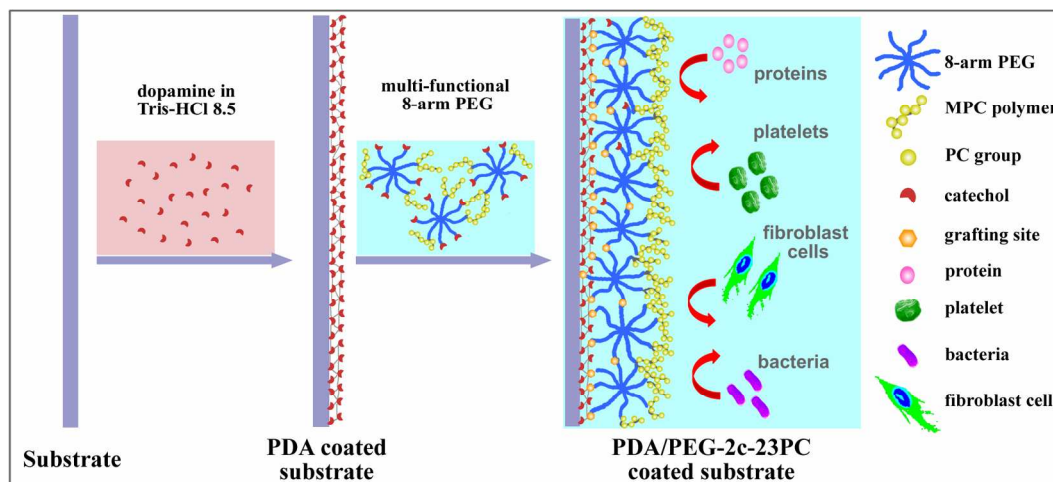


Fig. 9 Quantitative results of long-term attachment of *E. coli* (a), *P. aeruginosa* (b) and *S. aureus* (c) on surface-modified glass substrates obtained from ImageJ analysis. * $p < 0.05$, ** $p < 0.01$ and *** $p < 0.005$.



Scheme 1 The schematic illustration of coating construction and fouling resistance of the PDA-mediated PC and catechol end-capped 8-arm PEG coating.

this measurement, the anti-bacteria attachment efficiency of PEG-2c-23PC was as high as 85%.

The long-term (7 days) bacteria adhesion on the differently modified glass surfaces was shown in Fig. S5, S6 and S7 by representative fluorescence microscope images. The bare and PDA coated substrates were massively covered by the bacteria during the studied period. However, very few bacteria were attached on PDA/PEG-2c-23PC, PDA/PEG-6c-23PC and PDA/PEG-8c surfaces. As shown in Fig. 9, the adhesion of all

the bacteria was dramatically suppressed by 99% after contacted for 24 hours on both the PDA/PEG-2c-23PC and PDA/PEG-6c-23PC coating surfaces. The excellent anti-bacteria attachment performance of these simply self-anchoring polymer coatings was as good as that of chemically grafted zwitterionic polymer brushes.⁴⁴ More excitingly, the long-term bacteria-resistance of the PC and catechol doubly biomimetic 8-arm PEG surfaces after 7 day contact could inhibit 97% of the adhesions. The outstanding performance of PDA/PEG-2c-23PC

and PDA/PEG-6c-23PC coatings might be related to the dual functions of the cell outer membrane mimetic PC interface^{45,46} and the branched PEG layer^{47,48}. The biofouling resistance of the PDA-mediated PC and catechol end-capped 8-arm PEG coating was schematically illustrated in Scheme 1.

In the case of PC and catechol-grafted 8-arm PEG polymers, more catechol content in the polymer provided easier and stronger anchoring on a surface, and more PC groups endowed better biocompatibility of the coating. On the other hand, more catechol content in the coatings promoted the attachment of proteins, cells and bacteria in all of our results. This phenomenon was supported by protein folding and aggregation occurred on PDA surface.⁴⁹ Therefore, the catechol content in the water-soluble antifouling polymer should be appropriate, enough to immobilize the coating and as less as possible to keep strong resistance to biofouling. More importantly, the design of the doubly biomimetic 8-arm PEGs and the simple fabrication strategy of cell outer membrane mimetic, biocompatible and antifouling coatings on material-independent substrates by self-anchoring reported in this article, could be extended to other kinds of functionalities and the number of the end-capped functional groups could be adjusted to optimize the performance of the functionalized multi-armed polymer coating.

4. Conclusions

We have successfully synthesized a new family of PC and/or catechol end-capped 8-arm PEGs and developed a general surface coating strategy to improve surface biocompatibility and antifouling properties. The partially grafted catechol groups could immobilize the modified 8-arm PEGs on a surface from solution, and the anchoring interaction could be enhanced by either increasing the catechol content of the polymer or precoating the substrate with polydopamine, which formed automatically from a dopamine solution onto almost all substrates including polytetrafluoroethylene. Meanwhile, the grafted PC groups at other ends of the anchored multi-arm PEGs formed cell outer membrane mimetic PC layer, which provided strong resistance to biofouling. The end-capped functional groups on the branched 8-arm PEGs could be adjusted to optimize the performance of coatings. The anti-biofouling property of the optimized self-anchoring PDA/PEG-2c-23PC coating was as excellent as that of a chemically grafted zwitterionic polymer brushes. This PDA-assisted immobilization for highly hydrophilic and function-adjustable multi-arm PEGs provides a universal and convenient way to fabricate a biocompatible and fouling-resistant surface, which hopefully can offer great opportunities to improve the biocompatibility and functions of host substrates for both biomedical and non-biomedical applications.

Acknowledgements

This work was supported by the National Natural Science Foundation of China (Nos. 20974087, 21244001, 21374087),

and the Fund of Engineering Laboratory of Xi'an City (No. 2012-12).

Notes and references

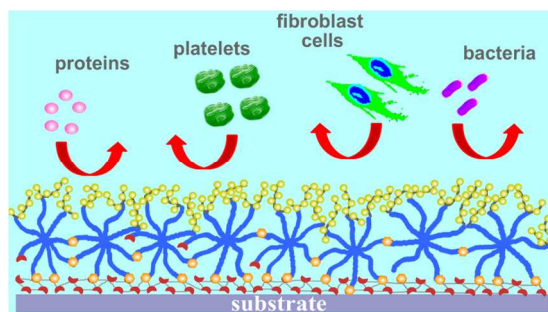
Key Laboratory of Synthetic and Natural Functional Molecule Chemistry of Ministry of Education, College of Chemistry and Materials Science, Northwest University, Xi'an 710127, Shaanxi, PR China. Email: gongyk@nwu.edu.cn, Tel: (86) 29 81535032, Fax: (86) 29 81535026.

† Electronic Supplementary Information (ESI) available: 1H NMR spectra of PMEN copolymer (Fig. S1), Static contact angle and XPS survey spectra of PEG-2c-23PC coated substrates (Fig. S2), Relative cell viability of L929 (Fig. S3), Quantitative results of L929 fibroblast cell attachments on five surface-modified glass substrates (Fig. S4), Fluorescence microscopic images of *E. coli*, *P. aeruginosa* and *S. aureus* contacted with differently modified glass substrates after 1, 3 and 7 days (Fig. S5, S6, S7). See DOI: 10.1039/b000000x/

- 1 K. A. Pollack, P. M. Imbesi, J. E. Raymond and K. L. Wooley, *ACS Appl. Mater. Interfaces*, 2014, **6**, 19265.
- 2 K. L. Prime and G. M. Whitesides, *Science*, 1991, **252**, 1164.
- 3 G. Cheng, H. Xue, Z. Zhang, S. Chen and S. Y. Jiang, *Angew. Chem. Int. Edit.*, 2008, **47**, 8831.
- 4 W. Lin, G. Ma, F. Ji, J. Zhang, L. Wang, H. Sun and S. Chen, *J. Mater. Chem. B*, 2015, **3**, 440.
- 5 N. Y. Kostina, S. Sharifi, A. S. Pereira, J. Michálek, D. W. Grijpmab and C. Rodriguez-Emmenegger, *J. Mater. Chem. B*, 2013, **1**, 5644.
- 6 S. Chen and S. Y. Jiang, *Adv. Mater.*, 2008, **20**, 335.
- 7 W. Zhao, Q. Ye, H. Hu, X. Wang and F. Zhou, *J. Mater. Chem. B*, 2014, **2**, 5352.
- 8 R. Zhou, P. F. Ren, H. C. Yang and Z. K. Xu, *J. Membr. Sci.*, 2014, **466**, 18.
- 9 A. J. Morse, S. Edmondson, D. Dupin, S. P. Armes, Z. Zhang, G. J. Leggett, R. L. Thompson and A. L. Lewis, *Soft Matter*, 2010, **6**, 1571.
- 10 D. Tan, Z. Li, X. Yao, C. Xiang, H. Tan and Q. Fu, *J. Mater. Chem. B*, 2014, **2**, 1344.
- 11 J. D. Andrade and V. Hlady, *Adv. Polym. Sci.*, 1986, **79**, 1.
- 12 S. I. Jeon, J. H. Lee, J. D. Andrade and P. G. Degannes, *J. Colloid Interface Sci.*, 1991, **142**, 149.
- 13 H. S. Kim, H. O. Ham, Y. J. Son, P. B. Messersmith and H. S. Yoo, *J. Mater. Chem. B*, 2013, **1**, 3940.
- 14 L. A. Tessler, C. D. Donahoe, D. J. Garcia, Y. S. Jun, D. L. Elbert and R. D. Mitra, *J. R. Soc. Interface*, 2011, **8**, 1400.
- 15 S. F. Chen, J. Zheng, L. Y. Li and S. Y. Jiang, *J. Am. Chem. Soc.*, 2005, **127**, 14473.
- 16 P. Liu, Q. Chen, L. Li, S. Lin and J. Shen, *J. Mater. Chem. B*, 2014, **2**, 7222.
- 17 S. Yang, S. P. Zhang, F. M. Winnik, F. Mwale and Y. K. Gong, *J. Biomed. Mater. Res. A*, 2008, **84**, 837.
- 18 N. Hao, Y. B. Wang, S. P. Zhang, S. Q. Shi, K. Nakashima and Y. K. Gong, *J. Biomed. Mater. Res. A*, 2014, **102**, 2972.
- 19 M. Tanaka, T. Sawaguchi, Y. Sato, K. Yoshioka and O. Niwa, *Tetrahedron Lett*, 2009, **50**, 4092.
- 20 Y. Iwasaki, A. Yamasaki and K. Ishihara, *Biomaterials*, 2003, **24**, 3599.

- 21 L. J. Liu, C. A. Burnyeat, R. S. Lepsenyi, I. O. Nwabuko and T. L. Kelly, *Chem. Mater.*, 2013, **25**, 4206.
- 22 V. Zoulalian, S. Monge, S. Zuercher, M. Textor, J. J. Robin and S. J. Tosatti, *J. Phys. Chem. B*, 2006, **110**, 25603.
- 23 D. Stanicki, S. Boutry, S. Laurent, L. Wacheul, E. Nicolas, D. Crombez, L. V. Elst, D. L. J. Lafontaine and R. N. Muller, *J. Mater. Chem. B*, 2014, **2**, 387.
- 24 T. Fujie, H. Haniuda and S. Takeoka, *J. Mater. Chem.*, 2011, **21**, 9112.
- 25 J. H. Waite and M. L. Tanzer, *Science*, 1981, **212**, 1038.
- 26 H. Lee, S. M. Dellatore, W. M. Miller and P. B. Messersmith, *Science*, 2007, **318**, 426.
- 27 Y. K. Gong, L. P. Liu and P. B. Messersmith, *Macromol. Biosci.*, 2012, **12**, 979.
- 28 Y. D. Xu, W. Huang, G. Ren, S. B. Qi, H. Jiang, Z. Miao, H. G. Liu, E. Lucente, L. H. Bu, B. Z. Shen, A. Barron and Z. Cheng, *ACS Macro. Lett.*, 2012, **1**, 753.
- 29 K. Ishihara, T. Ueda and N. Nakabayashi, *Polym. J.*, 1990, **22**, 355.
- 30 T. Konno, J. Watanabe and K. Ishihara, *Biomacromolecules*, 2004, **5**, 342.
- 31 M. Gong, Y. B. Wang, M. Li, B. H. Hu and Y. K. Gong, *Colloids Surf. B*, 2011, **85**, 48.
- 32 T. J. Mosmann, *J. Immunol. Methods*, 1983, **65**, 55.
- 33 D. E. Fullenkamp, J. G. Rivera, Y. K. Gong, K. H. A. Lau, L. He, R. Varshney and P. B. Messersmith, *Biomaterials*, 2012, **33**, 3783.
- 34 H. S. Sundaram, X. Han, A. K. Nowinski, N. D. Brault, Y. Li, J. R. Ella-Menye, K. A. Amoaka, K. E. Cook, P. Marek, K. Senecal and S. Y. Jiang, *Adv. Mater. Interfaces*, DOI: 10.1002/admi.201400071.
- 35 T. Mutsuo, S. Takahiro, S. Yukari, Y. Kyoko and N. Osamu, *Tetrahedron Lett.*, 2009, **50**, 4092.
- 36 D. R. Dreyer, D. J. Miller, B. D. Freeman, B. D. D. R. Paul and C. W. Bielawski, *Langmuir*, 2012, **28**, 6428.
- 37 J. Liebscher, R. Mrówczyński, H. A. Scheidt, C. Filip, N. D. Hädäde, R. Turcu, A. Bende and S. Beck, *Langmuir*, 2013, **29**, 10539.
- 38 H. F. G. Heijnen, A. E. Schiel, R. Fijnheer, H. J. Geuze and J. J. Sixma, *Blood*, 1999, **94**, 3791.
- 39 K. Park, F. W. Mao and H. Park, *J. Biomed. Mater. Res.*, 1991, **25**, 407.
- 40 C. S. Zhao, X. D. Liu, M. Nomizu and N. Nishi, *Biomaterials*, 2003, **24**, 3747.
- 41 Q. Wei, B. Li, N. Yi, B. Su, Z. Yin, F. Zhang, J. Li and C. Zhao, *J. Biomed. Mater. Res. A*, 2011, **96**, 38.
- 42 P. H. Chua, K. G. Neoh, E. T. Kang and W. Wang, *Biomaterials*, 2008, **29**, 1412.
- 43 E. D. Giglio, L. Sabbatini, S. Colucci and G. Zamboni, *J. Biomat. Sci. Polym. E*, 2000, **11**, 1073.
- 44 J. Kuang and P. B. Messersmith, *Langmuir*, 2012, **28**, 7258.
- 45 Y. B. Wang, M. Gong, S. Yang, K. Nakashima and Y. K. Gong, *J. Membr. Sci.*, 2014, **452**, 29.
- 46 M. Gong, Y. Dang, Y. B. Wang, S. Yang, F. M. Winnik and Y. K. Gong, *Soft Matter*, 2013, **9**, 4501.
- 47 J. Groll, J. Fiedler, E. Engelhard, T. Ameringer, S. Tugulu, H. A. Klok, R. E. Brenner and M. Moeller, *J. Biomed. Mater. Res. A*, 2005, **74**, 607.
- 48 P. Gasteier, A. Reska, P. Schulte, J. Salber, A. Offenhäusser, M. Moeller and J. Groll, *Macromol. Biosci.*, 2007, **7**, 1010.
- 49 T. G. Hastings, *J. Bioenerg. Biomembr.*, 2009, **41**, 469.

Table of content



Phosphorylcholine and catechol doubly functionalized 8-arm PEGs simplify coating immobilization on material-independent substrates with improved biocompatibility.